Combustion and Flame 205 (2019) 1–6

Contents lists available at ScienceDirect

Combustion and Flame

journal homepage: www.elsevier.com/locate/combustflame

Observed dependence of characteristics of liquid-pool fires on swirl magnitude

Wilfried Coenen*, Erik J. Kolb, Antonio L. Sánchez, Forman A. Williams

Department of Mechanical and Aerospace Engineering, University of California San Diego, La Jolla, CA 92093-0411, USA

ARTICLE INFO

Article history:
Received 7 February 2019
Revised 17 March 2019
Accepted 22 March 2019

Keywords:
Fire whirls
Pool fires
Buoyant-plume stability
Vortex breakdown

ABSTRACT

One dozen vertically oriented thin rectangular vanes, 62 cm tall and 15.2 cm wide, were placed 27 cm from the center of heptane and ethanol pool fires in continuously fed, floor-flush pans 3.2 cm and 5.1 cm in diameter in the laboratory. The vanes were all oriented at the same fixed angles from the radial direction, for 9 different angles, ranging from 0° to 85°, thereby imparting 9 different levels of circulation to the air entrained by each pool fire. The different swirl levels were observed to engender dramatically different pool-fire structures. Moderate swirl suppresses the global puffing instability, replacing it by a global helical instability that generates a tall fire whirl, the height of which increases with increasing circulation. Except for the largest heptane pool, higher swirl levels produced vortex breakdown, resulting in the emergence of a bubble-like recirculation region with a ring vortex encircling the axis. Measured burning rates increase with increasing swirl levels as a consequence of the associated increasing inflow velocities reducing the thickness of the boundary layer within which combustion occurs right above the liquid surface, eventually forming detached edge flames in the boundary layer that move closer to the axis as the circulation is increased. Still higher circulation reduces the burning rate by decreasing the surface area of the liquid covered by the flame, thereby reducing the height of the fire whirl. Even higher circulation causes edge-flame detachment, resulting in formation of the blue whirl identified in recent literature, often meandering over the surface of the liquid in the present experiments. This sequence of events is documented herein.

1. Introduction

Aside from the inherent thermochemical and transport parameters associated with the fuel, the gas-phase motion induced by buoyancy, for an axisymmetric pool fire of a liquid contained in a round pool of radius a, is controlled by a single dimensionless number, the Rayleigh number $Ra = (ga^3)/(\nu D_T)$, defined here with use of the kinematic viscosity ν and thermal diffusivity D_T of the ambient air, with g denoting the gravitational acceleration; alternatively, the associated Grashof number $Gr = (ga^3)/\nu^2$ could have been selected, since the Prandtl number ν/D_T is practically constant. Imposition of circulation of air about the axis introduces a second controlling parameter, which may be taken to be the inlet angle α between the inward radial component of velocity and the circumferential component of velocity at a specified, geometrically similar, external location in the surrounding air. The purpose of the present investigation is to explore the influence of this second controlling parameter on the structure and dynamics of axisymmetric pool fires, thereby helping to improve our understanding of fire whirls, which have been thoroughly reviewed recently [1].

A distinctive characteristic of liquid-pool flames is their tendency to develop self-sustained oscillations, shedding large toroidal coherent structures at a well-defined frequency while maintaining axial symmetry, a phenomenon referred to in the literature as "puffing". It is well established that, under normal conditions of temperature and pressure, diffusion flames formed over hydrocarbon fuel pools larger than a few centimeters in diameter puff with a frequency on the order of $f \sim \sqrt{g/a}$ [2–5]. Despite earlier opinions to the contrary, favoring a convective instability [5], pool-fire puffing recently has been definitively shown [6] to correspond to a hydrodynamic global instability of the flow, the onset of which is associated with a critical value of the Rayleigh number.

The puffing phenomenon of pool fires is not seen in fire whirls, which exhibit quite different types of fluid flow [1], more closely resembling then flow in fully developed turbulent buoyant plumes. The entrainment rate of the turbulent plume developing above the flame, linearly proportional to the burning rate, increases with the two thirds power of the vertical distance, inducing in the

* Corresponding author.
E-mail address: wicoenen@ucsd.edu (W. Coenen).

https://doi.org/10.1016/j.combustflame.2019.03.032
0010-2180/

surrounding atmosphere a flow that is largely inviscid, with the exception of a thin boundary-layer region adjacent to the horizontal wall [7]. The deflection of the induced radial inflow at geometrical constraints found in the far field, such as vertical vanes in experiments or topographic features in wildland fires, may introduce an azimuthal velocity component, leading to the establishment of swirling motion. The centripetal acceleration of the resulting swirling flow, whose magnitude Γ^2/r^3 is proportional to the square of the flow circulation Γ and inversely proportional to the cube of the distance to the axis r, is balanced by the radial pressure gradient. Viscous forces slow down the swirling motion in a near-wall boundary layer, where the imposed pressure gradient generates a strong radial inflow with characteristic velocities v_r increasing on approaching the axis according to $v_r \sim \Gamma_o/r$, where Γ_o is the value of the circulation outside the boundary layer [8]. As suggested by previous experimental results [9], the collision of this wall jet over the fuel pool plays a key role in the formation of the columnar vortex at the base of the fire whirl.

A number of different approaches have been employed to generate fire whirls in the laboratory for visual observations and scientific measurements. The earliest design employed two slightly offset, vertically oriented, semi-cylindrical surfaces surrounding the pool that leave two small slits for the tangential inflow of the entrained air [10]. This configuration, which has often been used for scientific measurements, extending to recent times [11,12], or variations of it involving offset vertical planar walls, can be quite convenient but does not afford easy access to investigating effects of different inlet angles α. That angle can be easily adjusted if the circular walls are replaced by a rotating cylindrical screen [13], but that requires construction of a more elaborate, motor-driven apparatus. It is more convenient to employ a set of long vertical flow vanes placed at an adjustable angle with respect to the radial direction, as was done in an experimental study of dust devils [14]. This last approach is the one selected here. As a consequence of this selection, the results reported below, including the specific sequence of flow phenomena occurring for increasing α, pertain to fire whirls where the swirling motion is driven by plume entrainment, as often occurs in realistic scenarios, and might be different from those observed in experimental configurations involving rotating screens or tangential blowers, for example, for which the level of swirl attainable is independent of the near-axis flow entrainment.

Just as for any other slender swirling flow, dust devils and fire whirls may be subject to vortex breakdown [15,16] (an abrupt change in the flow structure with a very pronounced retardation of the streamwise flow leading to the formation of a stagnation point along the axis and a corresponding divergence of the stream surfaces). Recent experiments [17] have unveiled the existence of a new type of whirling flame, developing after vortex breakdown, with a fundamentally different structure consisting of a light blue inverted cone at the base, extending outward to a bright ring, followed by a purple haze above. This so-called *blue whirl* has been found as a transient object evolving naturally from a traditional fire whirl as the circulation is increased [18]. Its existence has been shown to rely on the presence of the recirculating-flow bubble that results from the vortex breakdown, which can develop only for sufficiently large ambient circulation [19]. All of these phenomena are encountered in the present study.

2. The experimental arrangement

In our experiments, the inclination angle α of the vanes with respect to the radial direction (see Fig. 1) is used as a direct controlling mechanism to set the level of ambient circulation, with $\Gamma \propto \tan\alpha$. The case $\alpha = 0$ corresponds to a swirl-free atmosphere, and it results in puffing flames whose stability characteristics have been studied recently [6]. For α close to $\alpha = 90^\circ$, the resulting outer flow conditions can be expected to approach those present in experiments using two slightly offset semi-cylindrical surfaces. The entire range of swirl levels and associated stationary swirling-flame solutions are to be explored here by sequentially modifying the value of α in a series of experiments for a given fuel and a given pool radius.

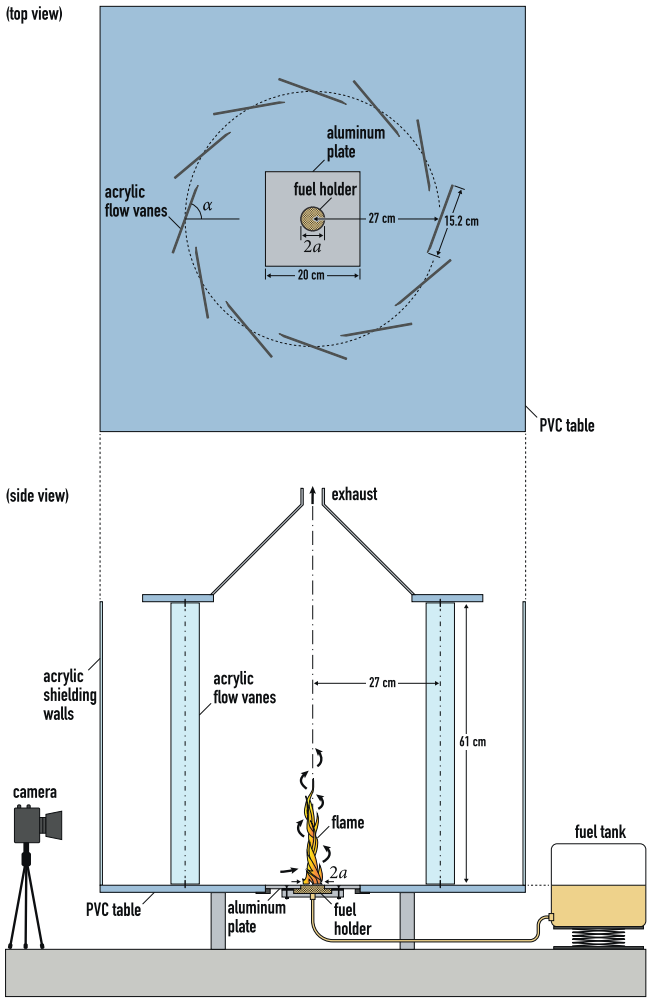

Fig. 1. Schematic view of the experimental setup used in this study.

The experimental facility, depicted in Fig. 1, was designed using as a basis the setup recently employed to study the onset of pool-fire puffing [6]. A set of twelve vertical acrylic vanes with a width of 15.2 cm and a height of 61 cm was placed at a large radial distance to deflect the radial air inflow induced by the entrainment of the flame and induce a swirling motion. Although this method has been employed to produce swirl in seminal experiments of dust-devil dynamics [14], it does not appear to have been employed in fire-whirl experiments. The angle of inclination of the vanes with respect to the radial direction, α, serves to control the level of swirl, as previously discussed. The burner, which sits in the center of a 90 cm × 90 cm × 12.7 mm PVC table, is composed of a 20 cm × 20 cm × 6.35 mm aluminum plate with a circular hole of diameter $2a = 32$ mm or $2a = 51$ mm in its center, and an aluminum fuel holder mounted underneath.

To prevent convective currents in the liquid fuel, the fuel holder is filled nearly to the rim with a layer of glass beads (3 mm in diameter). The fuel holder is connected to an external fuel tank with a cross-sectional area of approximately 350 $\text{cm}^2 \gg \pi a^2$. In this manner, once the height of the tank is adjusted so that the

burner is filled to the desired level with fuel, this level remains essentially constant during the course of a measurement (typically about five minutes). The external tank is placed on a high-precision load cell to allow measurement of the fuel-consumption rate.

External perturbations to the flame are minimized by surrounding the complete experiment with acrylic shielding walls, the volume between these walls and the vanes, as well as the opening at the top, being large enough that the air contained therein differs negligibly from that which would be present in a quiescent ambient atmosphere. The flame dynamics corresponding to a given swirl level was recorded with a Panasonic Lumix FZ300 camera at a frame rate of 120 fps. At each angle α, the flame is allowed to burn for a few minutes so that the system reaches a steady state before beginning simultaneous data acquisition of flame behavior and burning rate. The latter was obtained by averaging the fuel consumption over one-minute intervals, with differences in burning rates measured over consecutive intervals remaining always smaller than 5%, hence confirming the steady operation of the system.

3. Experimental results and discussion

3.1. Sample flame images and associated burning rate

Results were obtained for two fuel-pool diameters, $2a = 32$ mm ($Ra = 111,000$) and $2a = 51$ mm ($Ra = 451,000$), and values of the flow-vane inclination angle in the range from 0° to 85°. To test effects of radiant energy flux, experiments were conducted for two fuels with different sooting propensity, namely ethanol (low propensity) and heptane (high propensity). For the pool sizes considered, the resulting flames are always unsteady. A summary of sample flame instantaneous images, selected from the videos to illustrate the different flow phenomena occurring at each inclination angle, is presented in Fig. 2. As the inclination angle is increased, the flames are seen in this figure to experience transitions through a series of stages, each of which is described in the following subsections.

Figure 3 shows the measured fuel consumption rates associated with the experiments in Fig. 2. With increasing levels of ambient swirl (i.e. increasing values of the inclination angle α), the fuel consumption first increases, then reaches a maximum, beyond which it is seen to decrease again. The initial increase is associated with an increased rate of heat transfer to the fuel surface caused by the flame sheet lying closer to the fuel surface. The flame, attached to the rim of the pan, is in a boundary layer that becomes thinner as α increases. The final decrease in fuel-consumption rate is associated with a detachment of the flame edge from the rim, effectively reducing the rate of fuel vaporization (see Section 3.4). The higher burning rate of heptane than ethanol results from its higher heat-transfer rate.

3.2. Helical global modes

For both values of the fuel-pool diameters used in this set of experiments the associated Rayleigh numbers are supercritical in the absence of ambient circulation (i.e. for $\alpha = 0$), so that the resulting flame puffs in a nearly axisymmetric fashion, as predicted by the global instability analysis [6]. The global puffing instability is suppressed by the appearance of a stationary helical global instability as the level of swirl in the surrounding atmosphere increases for increasing α. A strong puffing-free fire whirl is eventually seen to form, around $\alpha \simeq 50^\circ$.

These observations indicate that the formation of a fire whirl requires a sufficient level of ambient swirl, corresponding to a sufficiently large value of the inclination angle α. This is consistent with the present knowledge of liquid-pool-fire stability. Thus, in the absence of ambient swirl, the global hydrodynamic instability of liquid-pool fires is dominated by the azimuthal mode number $m = 0$ (axisymmetric), the puffing mode [6], resulting in the puffing flame shown for $\alpha = 0$ in Fig. 2. Under these swirl-free conditions, values of $m \geq 1$ (helical) modes display lower growth rates and consequently play a secondary role in the resulting flame dynamics. The axisymmetric instability mode is also dominant in jet diffusion flames [20], low-density jets [21], and buoyant plumes [22,23].

The presence of ambient swirl may change this stability behavior. It may be expected that the growth rate of the axisymmetric ($m = 0$) and helical ($m \geq 1$) modes carries a dependence on the level of ambient swirl, additional to the dependence on the Rayleigh number Ra. The transition from puffing to whirling therefore is likely to be associated with the critical swirl level at which the growth rate of the helical mode (possibly $m = 1$) exceeds that of the axisymmetric mode. Global stability analyses accounting for the presence of ambient swirl, which are not yet available, would be needed to test this inference, providing accurate quantification of the transition conditions. It is known that such modes exist, but it has not been established that any of them can reach instability at lower Rayleigh numbers than that for the axial mode.

The higher ambient circulation associated with larger values of α is accompanied by a larger radial pressure gradient, which, in turn, accelerates radially the gas in the near-wall boundary-layer region surrounding the base of the fire. This affects the diffusion flame that develops from the pool rim, causing it to approach the fuel-pool surface, increasing the associated fuel vaporization rate and resulting in stronger fire whirls with larger heights.

3.3. Vortex breakdown

An additional increase of the inclination to $\alpha = 70^\circ$ further lengthens the fire whirl, with the resulting strong swirling motion leading to vortex breakdown of the columnar flame, indicated by the emergence of a bubble-like recirculating region (see Fig. 4). Although vortex breakdown has been known to be present in fire whirls [13] and dust devils [14], the specific conditions needed for its development and the resulting effects on the flow are still not fully understood. The associated problem, however, is fundamentally different from that of vortex breakdown in technological applications pertaining to combustion, in which the swirling motion is imparted in the jet stream [24], with the ratio of the fluxes of angular momentum to axial momentum defining a swirl number that characterizes vortex breakdown [15]. A critical swirl number of order unity defines in these combustors the transition from a slender jet to a vortex-breakdown flow with a stagnation point along the axis.

In contrast to swirl combustors, the definition of a swirl number determining the critical conditions for formation of vortex breakdown in fire whirls is not clear. For fire whirls, the breakdown bubble forms in the near-pool region where the incoming boundary-layer flows at all angles collide at the center to give an uprising jet flow [14]. The presence of a stagnation point deflecting the flow reduces the axial momentum flux, thereby limiting the resulting fire-whirl height, as shown in Fig. 4. Present experimental observations appear to indicate that the bubble moves towards the fuel-pool surface as the value of α is increased further. The conditions for vortex breakdown to occur in fire whirls, as well as the subsequent history of the breakdown bubble, are in need of further investigation. Such studies may clarify why breakdown did not occur for the larger heptane fire, which exhibited a substantially higher burning rate and radiant energy flux level, although breakdown may have been seen if it had been possible to place the vanes at a larger distance from the axis.

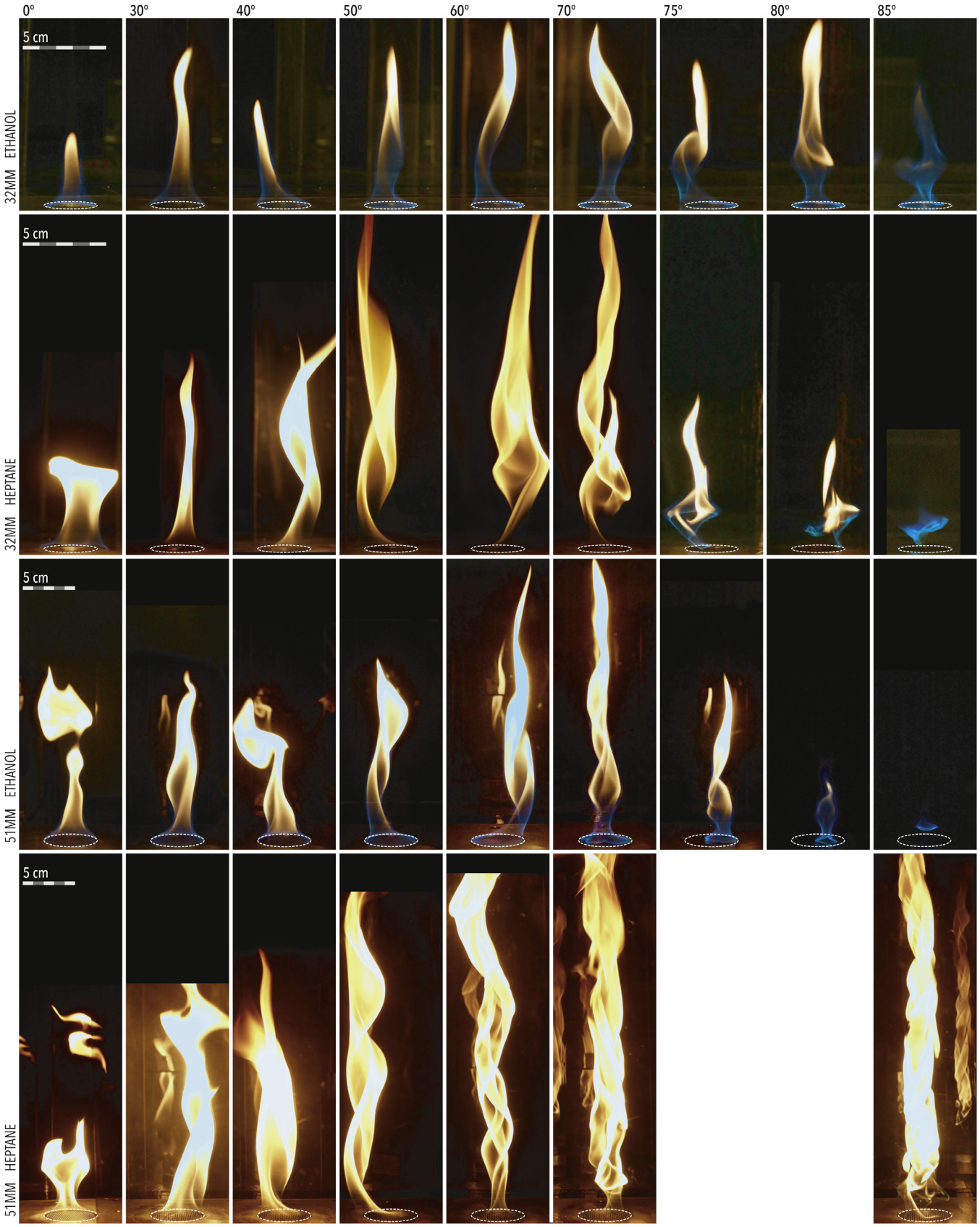

Fig. 2. Sample flame images for two fuels, two fuel-pool diameters, and a range of flow-vane inclination angles.

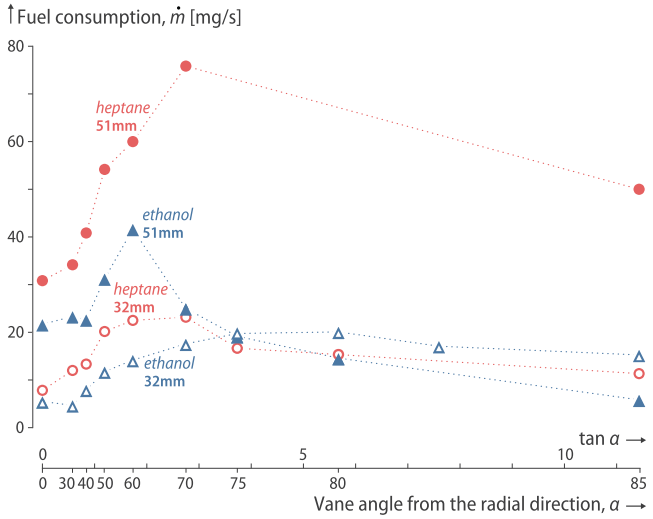

Fig. 3. Fuel consumption as a function of ambient swirl, for heptane and ethanol, and two different fuel-pool diameters. The experimental measurements, represented by symbols, are connected by dashed lines to facilitate visualization of the results.

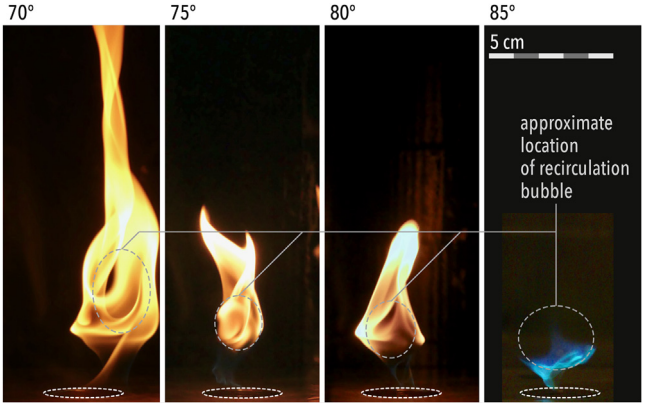

Fig. 4. The appearance of a recirculation bubble as a consequence of vortex breakdown, for heptane with a fuel-pool diameter $2a = 32$ mm.

3.4. Fire-whirl height reduction

The anchoring of the flame edge at the pool rim depends critically on the strain rate imposed by the incoming radial flow, with higher strain rates for increasing values of α. As explained in the introduction, the results of an early theoretical analysis pertaining to the boundary-layer flow induced by a potential vortex [8] suggest that the flow surrounding the fire whirl includes a near-wall radial jet with characteristic radial velocity $v_r \sim \Gamma_o/r$; the associated near-wall velocity gradients at first decrease with decreasing radius through boundary-layer growth, then reach a minimum, and finally increase according to $\sim \Gamma_o/r^2$ as the radius approaches zero, where Γ_o is the value of the circulation at the outer edge of the boundary layer. As can be expected from edge-flame theory [25], the flame may remain attached provided that the strain rate at the rim of the fuel pool, of order Γ_o/a^2, does not exceed a critical value, given in order of magnitude by the inverse of the residence time across the stoichiometric planar deflagration [25]. Since in the experiments $\Gamma_o \propto \tan\alpha$, a sufficiently large value of α should cause detachment of the edge flame from its near-rim anchoring region. The location of the flame edge over the fuel surface after detachment becomes determined by a balance between the edge flame-spread propagation velocity [26,27] and the boundary-layer radial inflow.

As can be seen in Fig. 2, all flames with $\alpha \leq 60°$ remain attached. For larger values of α the edge flame recedes from the pool edge, moving radially inward to a location over the fuel-pool surface where it encounters a lower strain rate, as seen for $\alpha = 70°$ and, more clearly, for $\alpha = 75°$. The reduced extent of the flame base results in a smaller global fuel-vapor vaporization rate, significantly limiting the height of the associated flame, as seen most dramatically in the flow established for $\alpha = 80°$. The resulting shortened fire whirl moves continuously around the axis as the edge-flame wanders in response to the boundary-layer flow in these experiments. Although differently designed experiments might eliminate this wandering, there is nothing in the present tests that could stabilize whatever in-plane instabilities promote the observed meander.

Shown in Fig. 5 are close-up views at the base of the larger of the two ethanol fires, for conditions corresponding to the last five angles of Fig. 2. In the first frame at the left, with $\alpha \simeq 60°$, the flame is seen to remain attached to the edge of the pool, the strain rate there being insufficient to produce detachment. In the second picture from the left, for $\alpha \simeq 70°$, the edge flame is seen to begin to recede from the pool rim. The last three photographs, from 75° to 85°, document how the flame eventually begins to lift up out of the boundary layer as the circulation is increased.

3.5. Flame lift-off and transition to blue whirl

After the edge flame lifts up from the pool surface, the presence of the stagnation point near the bottom of the vortex-breakdown recirculating bubble enables it to stabilize at a new location, leading to the formation of a lifted partially premixed front belonging to the blue-whirl family [17–19,28]. Although the shape of the resulting front is drastically different from that of triple flames propagating along mixing layers, it can be conjectured that the light blue cone at the base (present even in the far-right frame of the

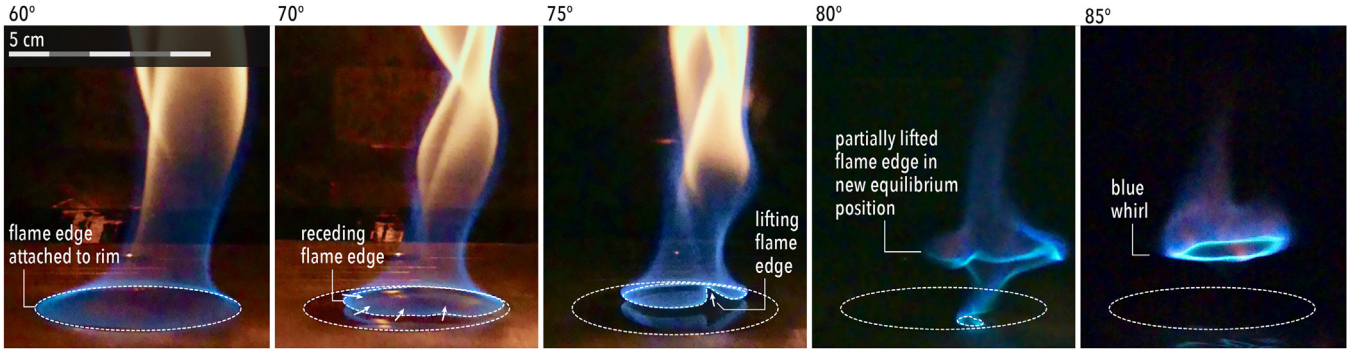

Fig. 5. Detachment of the flame edge from the rim, lifting of the flame edge, and the formation of a blue whirl, for ethanol with a fuel-pool diameter $2a = 51$ mm.

figure but essentially impossible to see because of excessively weak blue emissions) corresponds to a rich branch, the bright ring identifies the stoichiometric point, and the purple haze above is the lean flame, which curves inwards in response to the surrounding radial velocity. Since the flame is lifted from the surface, the effect of heat conduction to the fuel is necessarily limited. Hence, with radiation being also unimportant in these soot-free flames, convection appears to be the only effective mechanism transferring heat from the flame front to the fuel surface. This observation further underscores the importance of the flow structure in the collision region at the base of the flame [14].

4. Conclusions

It is noteworthy that the relatively simple apparatus described here can produce such a wide variety of pool-fire and fire-whirl phenomena, merely by varying the single entry-angle parameter α. The experimental observations reported here help to improve our understanding of fire-whirl phenomena, although it should be abundantly clear from the preceding discussion that much more research is needed to obtain good quantitative knowledge of these intriguing phenomena.

References

[1] A. Tohidi, M.J. Gollner, H. Xiao, Fire whirls, Annu. Rev. Fluid Mech. 50 (2018) 187–213.
[2] H.W. Emmons, Scientific progress on fire, Annu. Rev. Fluid Mech. 12 (1980) 223–236.
[3] G. Heskestad, Dynamics of the fire plume, Phil. Trans. R. Soc. A 356 (1748) (1998) 2815–2833.
[4] P. Joulain, The behavior of pool fires: state of the art and new insights, Symp. (Int.) Combust. 27 (1998) 2691–2706.
[5] S.R. Tieszen, On the fluid mechanics of fires, Annu. Rev. Fluid Mech. 33 (2001) 67–92.
[6] D. Moreno-Boza, W. Coenen, J. Carpio, A.L. Sánchez, F.A. Williams, On the critical conditions for pool-fire puffing, Combust. Flame 192 (2018) 426–438.
[7] J.S. Turner, Buoyant plumes and thermals, Annu. Rev. Fluid Mech. 1 (1969) 29–44.
[8] O.R. Burggraf, K. Stewartson, R. Belcher, Boundary layer induced by a potential vortex, Phys. Fluids 14 (9) (1971) 1821–1833.
[9] R. Dobashi, T. Okura, R. Nagaoka, Y. Hayashi, T. Mogi, Experimental study on flame height and radiant heat of fire whirls, Fire Technol. 52 (4) (2016) 1069–1080.
[10] G.M. Byram, R.E. Martin, Fire whirlwinds in the laboratory, Fire Control Notes 33 (1) (1962) 13–17.
[11] K.A. Hartl, A.J. Smits, Scaling of a small scale burner fire whirl, Combust. Flame 163 (2016) 202–208.
[12] K. Kuwana, S. Morishita, R. Dobashi, K.H. Chuah, K. Saito, The burning rate's effect on the flame length of weak fire whirls, Proc. Combust. Inst. 33 (2011) 2425–2432.
[13] H.W. Emmons, S.-J. Ying, The fire whirl, Proc. Combust. Inst. 11 (1967) 475–488.
[14] J.B. Mullen, T. Maxworthy, A laboratory model of dust devil vortices, Dyn. Atmos. Oceans 1 (3) (1977) 181–214.
[15] M.G. Hall, Vortex breakdown, Annu. Rev. Fluid Mech. 4 (1) (1972) 195–218.
[16] M. Escudier, Vortex breakdown: observations and explanations, Progr. Aerosp. Sci. 25 (2) (1988) 189–229.
[17] H. Xiao, M.J. Gollner, E.S. Oran, From fire whirls to blue whirls and combustion with reduced pollution, Proc. Nat. Acad. Sci. 113 (34) (2016) 9457–9462.
[18] S.B. Hariharan, E.T. Sluder, M.J. Gollner, E.S. Oran, Thermal structure of the blue whirl, Proc. Combust. Inst. 37 (3) (2018) 4285–4293.
[19] Y. Hu, S.B. Hariharan, H.T. Qi, M.J. Gollner, E.S. Oran, Conditions for formation of the blue whirl, Combust. Flame (2019) submitted.
[20] D. Moreno-Boza, W. Coenen, A. Sevilla, J. Carpio, A.L. Sánchez, A. Liñan, Diffusion-flame flickering as a hydrodynamic global mode, J. Fluid Mech. 798 (2016) 997–1014.
[21] W. Coenen, L. Lesshafft, X. Garnaud, A. Sevilla, Global instability of low-density jets, J. Fluid Mech. 820 (2017) 187–207.
[22] K.K. Bharadwaj, D. Das, Global instability analysis and experiments on buoyant plumes, J. Fluid Mech. 822 (2017) 97–145.
[23] R.V.K. Chakravarthy, L. Lesshafft, P. Huerre, Global instability of buoyant jets and plumes, J. Fluid Mech. 835 (2018) 654–673.
[24] S. Candel, D. Durox, T. Schuller, J.-F. Bourgouin, J.P. Moeck, Dynamics of swirling flames, Annu. Rev. Fluid Mech. 46 (2014) 147–173.
[25] A. Liñán, M. Vera, A.L. Sánchez, Ignition, liftoff, and extinction of gaseous diffusion flames, Annu. Rev. Fluid Mech. 47 (2015) 293–314.
[26] T. Hirano, K. Saito, Fire spread phenomena: the role of observation in experiment, Prog. Energy Combust. Sci. 20 (6) (1994) 461–485.
[27] H.D. Ross, Ignition of and flame spread over laboratory-scale pools of pure liquid fuels, Prog. Energy Combust. Sci. 20 (1) (1994) 17–63.
[28] S.B. Hariharan, P. Anderson, H. Xiao, M.J. Gollner, E.S. Oran, The blue whirl: boundary layer effects, temperature and OH* measurements, Combust. Flame 203 (2019) 352–361.